

¹Institute for Mathematics and its Applications, University of Minnesota, Minneapolis

²Dept. of Mathematics and School of Computational Science and Information Technology,
Florida State University, Tallahassee

Adaptive observations in the context of 4D-Var data assimilation

D. N. Daescu¹ and I. M. Navon²

With 14 Figures

Received August 5, 2002; accepted January 17, 2003

Published online: July 1, 2003 © Springer-Verlag 2003

Summary

The design of adaptive observations strategies must account for the particular properties of the data assimilation method. A new adjoint sensitivity approach to the targeted observations problem is proposed in the context of four-dimensional variational data assimilation (4D-Var). The method is based on a periodic update of the adjoint sensitivity field that takes into account the interaction between time distributed adaptive and routine observations. Information provided by all previously located observations is used to identify best locations for new targeted observations. Adaptive observations at distinct instants in time are selected in a sequential manner such that the method is only suboptimal. The selection algorithm proceeds backward in time and requires only one additional adjoint model integration in the assimilation window. Therefore, the method is very efficient and is suitable for practical applications. A comparative performance analysis is presented using the traditional adjoint sensitivity method as well as the total energy singular vectors technique as alternative adaptive strategies. Numerical experiments are performed in the twin experiments framework using a two-dimensional global shallow water model in spherical coordinates and an explicit Turkel-Zwas discretization scheme. Data from a NASA 500 mb analysis valid for 00Z 16 Mar 2001 6 h obtained with the GEOS-3 model was used to specify the geopotential height at the initial time and the initial velocities were obtained from a geostrophic balance. Numerical results show that the new adaptive observations approach is a promising method for targeted observations and its implementation is feasible for large scale atmospheric models.

1. Introduction

Short term prediction of rapidly evolving meteorological events may be greatly improved by reducing the analysis errors in dynamically sensitive geographical regions. Adaptive (targeted) observations strategies aim to improve the forecast of numerical weather prediction (NWP) models by identifying optimal locations where additional observations resources must be allocated. The significant research dedicated recently to the adaptive observations problem is primarily motivated by the fact that forecast failure of severe weather events (e.g., hurricane) may have dramatic economical and societal impacts. At the same time, the expansion of the current observational network and the design of future observing networks require an assessment of the value added by observational data to improve the model's forecast. Finding the best cost-effective methods for improving the forecast skill remains a practical problem of major importance. Expensive field-deployed resources can be utilized more effectively and the science success can be maximized by selecting an optimal observational network.

Mathematical framework and a rigorous statistical formulation of the adaptive observation

problem is described by Berliner et al (1999). However, implementation of optimal statistical methods may not be feasible in practice due to the difficulty to provide accurate estimates of the model and observational errors statistics, the large dimension of the state space used in NWP ($\sim 10^7$), and limited computational resources. Recent field experiments such as FASTEX (Joly et al, 1999), NORPEX (Langland et al, 1999) and WSRP (Szunyogh et al, 2001) provided real life applications where several feasible methods for adaptive observations were tested. An overview of the activities related to the use of targeted observations at the National Centers for Environmental Prediction (NCEP), including a discussion of the economic value of targeted observations, is presented in the review paper of Toth et al (2002).

The main differences between the proposed targeting strategies consist in the sensitivity analysis technique used to identify the areas where the errors in the initial conditions are rapidly growing and will mostly influence the forecast over the verification domain.

Adjoint modeling has been proved to be an essential tool for developing adaptive observations strategies. The adjoint of the tangent linear model associated with the nonlinear forecast model was used to implement targeting methods using the dominant singular vectors (Palmer et al, 1998; Buizza and Montani, 1999), gradient (adjoint sensitivity) fields (Langland et al, 1999; Langland and Rohaly, 1996) and sensitivity to observations (Baker and Daley, 2000; Doerenbecher and Bergot, 2001). Pu and Kalnay (2000) use the adjoint modeling and a quasi-inverse linear model approach (Kalnay et al, 2000) for targeting observations. A comparative analysis between targeted observations using the total energy singular vectors (TESV) and Hessian singular vectors (HSV) is presented in the recent work of Leutbecher et al (2002).

The Ensemble Transform (ET) (Bishop and Toth, 1999) and the Ensemble Transform Kalman Filter (ET KF) (Bishop et al, 2001) are adaptive techniques based on nonlinear ensemble forecasts. A comparison between the TESV and ET KF targeting methods is presented by Majumdar et al (2002).

Despite recent advances in the theoretical formulation and implementation of targeting

methods, the problem of the optimal adaptive sampling is a young discipline and many open questions remain to be addressed. Studies performed during the field experiments revealed the potential benefits that may be achieved using adaptive observations as well as various practical issues and shortcomings of the current targeting methodologies. The adaptive methods may be effective as long as the linearization of the nonlinear dynamical model along a control trajectory remains valid. Since in practical applications the verification time is selected at a 24 h to 72 h range, it is essential to establish the validity of the linear approximation before these methods can be efficiently used (Hansen and Smith, 2000). The design of adaptive strategies must account for various factors such as: the forecast model details, the magnitude of the uncertainty in the initial conditions (Lorenz and Emanuel, 1998), the uncertainty growth (Rabier et al, 1996), the data assimilation scheme used to provide the initial conditions (Bergot, 2001), the configuration of the existing observational network (Morss et al, 2001), and the number of the additional observational resources to be allocated.

The characteristics of the data assimilation system may be integrated in the adaptive observations method by using the sensitivity to observations technique proposed by Baker and Daley (2000). This approach was studied for 3D-Var data assimilation by Doerenbecher and Bergot (2001) who emphasized that to optimize the efficiency of adaptive techniques the assimilation of both conventional and adaptive observations must be considered.

In this paper we investigate the design of an adaptive observations system given the configuration of the conventional observational network and assuming that four-dimensional variational data assimilation (4D-Var) is performed. The TESV and ET KF targeting methods were considered in the 4D-Var context by Leutbecher et al (2002) using a perfect model scenario and assuming that adaptive observations are available only in the middle of the assimilation period. Our work represents a first attempt to fully account for the temporal dimension of the 4D-Var scheme by considering time distributed adaptive observations. In particular, we show that the interaction between routine (fixed location) and targeted observations taken at distinct

instants in time plays a significant role in the efficiency of the adaptive strategy. We design a simple mechanism to account for the interdependence between space and time distributed observations and further use it to implement an adjoint based targeting method. A comparative study with the traditional adjoint sensitivity (AS) and TESV methods is performed using a shallow water model. Our preliminary results indicate that at a relatively low additional computational cost, as compared to the AS method, the benefits of the new proposed targeting method on forecast error reduction may be significant.

The paper is organized as follows: in Sect. 2 we formulate the adaptive observations problem in the 4D-Var data assimilation context. The two-dimensional shallow-water model used in the numerical experiments is presented in Sect. 3. An idealized framework (twin experiments) is used to implement the data assimilation procedure by considering a truth and a control experiment. In this way we assume that the forecast error is only due to the misspecification of the initial conditions. ‘‘Observations’’ are selected from the truth experiment state trajectory and are assimilated with 4D-Var using the initial conditions of the control experiment as background. In Sect. 4, we briefly review the AS and TESV methods for targeting observations. The interaction mechanism between time distributed adaptive observations and fixed location observations is described in Sect. 5. A new adjoint-based targeting method using interactive adjoint sensitivity (IAS) fields is presented. In Sect. 6, we perform a comparative performance analysis between IAS, AS, and TESV targeting methods in two different scenarios: first, we assume that the adaptive observations are the only available observations to the data assimilation system; second, fixed location observations distributed on a sparse uniform sub-grid are also included into the analysis. Concluding remarks and further research directions are presented in Sect. 7.

2. 4D-Var data assimilation and adaptive observations

Bergot (2001) studied the efficiency of adaptive observations using incremental 3D-Var and incremental 4D-Var data assimilation schemes (Courtier et al, 1994). The results obtained for

a SV targeting method demonstrate that the sampling of the sensitive area and the assimilation scheme are intimately dependent. In this section, we formulate the adaptive observations problem in the 4D-Var data assimilation context. We assume that a model forecast $\mathbf{x}^f = \mathcal{M}(\mathbf{x}^b)$ initiated at time t_0 from a background estimate \mathbf{x}^b of the true atmospheric state \mathbf{x}_0^t predicts a severe weather event at a future verification time $t_v > t_0$ over the verification domain \mathcal{D}_v .

In the analysis time interval $[t_0, T]$, $T < t_v$ the conventional observing network provides a set of time distributed observations \mathcal{O}^f . We will refer to \mathcal{O}^f as routine (fixed location) observations and the location of \mathcal{O}^f is a priori known at the initial time t_0 . In practical applications the length of the assimilation window $[t_0, T]$ is usually 6h, whereas the verification time t_v is selected at 24h to 72h range from t_0 . We assume that at each time instant t_i , $t_0 < t_i \leq T$, $i = 1, 2, \dots, I$ a number of n_i additional observational resources may be deployed. We will refer to these additional observations as adaptive observations, \mathcal{O}_i^a , as their location may be selected in a flexible manner and it may change from one time instant to another. The observational data $\mathcal{O} = \{\mathbf{x}^o\}$ available over the assimilation window has therefore two components $\mathcal{O} = \mathcal{O}^f \cup \mathcal{O}^a$, where $\mathcal{O}^a = \{\mathcal{O}_1^a, \mathcal{O}_2^a, \dots, \mathcal{O}_I^a\}$ is the adaptive observational path to be determined.

4D-Var data assimilation provides an optimal estimate \mathbf{x}_0^a of the true initial state \mathbf{x}_0^t as the solution of the minimization problem

$$\mathcal{J}(\mathbf{x}_0) = \mathcal{J}^b + \mathcal{J}^o, \quad \mathcal{J}(\mathbf{x}_0^a) = \min_{\mathbf{x}_0} \mathcal{J}(\mathbf{x}_0), \quad (1)$$

where \mathcal{J}^b is a measure of the distance of the initial state from the background estimate and \mathcal{J}^o is a measure of the distance between the model trajectory and observations over the assimilation window. The reader should refer to the work of Jazwinski (1970), and Daley (1991) for a detailed description of the various assumptions used by the data assimilation techniques, including a continuum formulation and the probabilistic interpretation.

Using adaptive observations and by performing data assimilation, we aim to reduce the error of some aspect of the forecast at the verification time on the verification domain which may be expressed as

$$\mathcal{J}_v(\mathbf{x}_0) = \frac{1}{2} \langle \mathbf{P}(\mathbf{x}_v^f - \mathbf{x}_v^{ref}), \mathbf{P}(\mathbf{x}_v^f - \mathbf{x}_v^{ref}) \rangle_C, \quad (2)$$

where $\mathbf{x}_v^f = \mathcal{M}(\mathbf{x}_0)$, \mathbf{x}_v^{ref} is the verifying analysis at t_v , and \mathbf{P} is a diagonal projection operator on \mathcal{D}_v satisfying $\mathbf{P}^* \mathbf{P} = \mathbf{P}^2 = \mathbf{P}$. The inner product $\langle \cdot, \cdot \rangle_C$ is defined as $\langle \mathbf{y}, \mathbf{z} \rangle_C = \langle \mathbf{y}, \mathbf{Cz} \rangle$ where \mathbf{C} is a symmetric positive definite matrix. In practice the total energy norm is often used to measure the forecast error (2).

The adaptive observations problem is now formulated as follows: find an adaptive observational path $\mathcal{O}^a = \{\mathcal{O}_1^a, \mathcal{O}_2^a, \dots, \mathcal{O}_I^a\}$ such that the solution \mathbf{x}_0^a of the corresponding 4D-Var data assimilation (1) minimizes the forecast error expressed by the functional (2).

In previous studies only one targeting time t_i was taken into consideration ($I=1$). Our problem formulation takes fully into account the temporal dimension of the 4D-Var scheme by considering multiple targeting instances (i.e., $I > 1$) in the assimilation window.

3. The model and the data assimilation procedure

The numerical experiments and the analysis presented in this paper were performed in the twin experiments framework using a global two-dimensional shallow-water model. The selection of this model is motivated by the fact that the shallow water equations (SWEs) serve as a first prototype of the partial differential equations describing the horizontal dynamics of the atmosphere and have been widely used by the atmospheric modeling community as a tool for testing promising numerical methods for solving atmospheric and oceanic problems. The simplicity of the SWEs facilitates a thorough investigation of the numerical methods and their complexity (Williamson et al, 1992) while capturing important characteristics present in more comprehensive atmospheric models.

3.1 Model description

In spherical coordinates, the dynamical equations are written

$$\begin{aligned} \frac{\partial u}{\partial t} + \frac{1}{a \cos \theta} \left[u \frac{\partial u}{\partial \lambda} + v \cos \theta \frac{\partial u}{\partial \theta} \right] \\ - \left(f + \frac{u}{a} \tan \theta \right) v + \frac{g}{a \cos \theta} \frac{\partial h}{\partial \lambda} = 0, \end{aligned} \quad (3)$$

$$\begin{aligned} \frac{\partial v}{\partial t} + \frac{1}{a \cos \theta} \left[u \frac{\partial v}{\partial \lambda} + v \cos \theta \frac{\partial v}{\partial \theta} \right] \\ + \left(f + \frac{u}{a} \tan \theta \right) u + \frac{g}{a} \frac{\partial h}{\partial \theta} = 0, \end{aligned} \quad (4)$$

$$\frac{\partial h}{\partial t} + \frac{1}{a \cos \theta} \left[\frac{\partial}{\partial \lambda} (hu) + \frac{\partial}{\partial \theta} (hv \cos \theta) \right] = 0, \quad (5)$$

where $f = 2\Omega \sin \theta$ is the Coriolis parameter, Ω is the angular speed of the rotation of the earth, h is the height of the homogeneous atmosphere, u and v are the zonal and meridional wind components, respectively, θ and λ are the latitudinal and longitudinal directions, respectively, a is the radius of the earth, and g is the gravitational constant.

The software developed by Giraldo and Neta (1995) was used to implement the forward model integration. We consider a discretization on a 72×36 grid ($5^\circ \times 5^\circ$) such that the dimension of the discrete state vector $\mathbf{x} = (h, u, v)$ is 7776. The model is integrated for 24 h using an explicit Turkel-Zwas scheme (Navon and de Villiers, 1987; Neta et al, 1997) and a Robert filtering using a Laplacian type time-diffusion term is performed for both spatial and temporal smoothing. To maintain numerical stability, the integration time step is limited to $\Delta t = 200$ s. Data obtained from a 500 mb analysis valid for 00Z 16 March 2001 6 h using the GEOS-3 model ($1.25^\circ \times 1^\circ$) was used to specify the geopotential height at the initial time t_0 and the initial velocity fields were obtained from a geostrophic approximation. The model state at the initial time and after a 24 h integration are displayed in Fig. 1.

3.2 The twin experiments framework

The data assimilation procedure and the impact of the adaptive observations are analyzed using a perfect model scenario. We will assume that the initial conditions described in the previous section represent the true (reference) atmospheric state \mathbf{x}_0^{ref} and the model trajectory $\mathbf{x}^{ref}(t)$ obtained during the reference run is used to provide observations. A background field is prescribed using a 5% random perturbation in the reference initial velocities. In a more realistic data assimilation environment, bred vectors obtained from the ensemble forecasts may be used to reflect the uncertainty in the initial conditions and to

estimate the background error covariance matrix (Kalnay, 2002; Corazza et al, 2002).

A forecast initiated at t_0 from the background estimate reveals large errors at the verification time $t_v = 24$ h over the spatial domain $\mathcal{D}_v = [125^\circ \text{E } 175^\circ \text{E}] \times [80^\circ \text{S } 40^\circ \text{S}]$ which is thus selected as the verification domain. In Figs. 2 and 3, we show the errors in the background field and the 24 h forecast, respectively, evaluated in the total energy norm

$$\langle \delta \mathbf{x}(\lambda, \theta), \delta \mathbf{x}(\lambda, \theta) \rangle = \frac{1}{2} ((\delta u)^2 + (\delta v)^2) + \frac{g}{h_0} (\delta h)^2, \quad (6)$$

where $\delta \mathbf{x}(\lambda, \theta) = \mathbf{x}(\lambda, \theta) - \mathbf{x}^{ref}(\lambda, \theta)$.

4D-Var data assimilation is performed in the assimilation window $[0 - 6]$ h and we assume that routine observations are available at $t = 6$ h only on a coarse $20^\circ \times 20^\circ$ mesh grid. The error in the forecast initiated from the analysis obtained with the data assimilation using routine observations is shown in Fig. 4. We notice that the overall quality of the forecast is improved over the entire domain. However, the forecast error over the domain of interest, \mathcal{D}_v , remains relatively large. To further improve the forecast over \mathcal{D}_v , we assume that each hour in the interval $[0 - 6]$ h five adaptive observations may be taken and their optimal location must be determined by

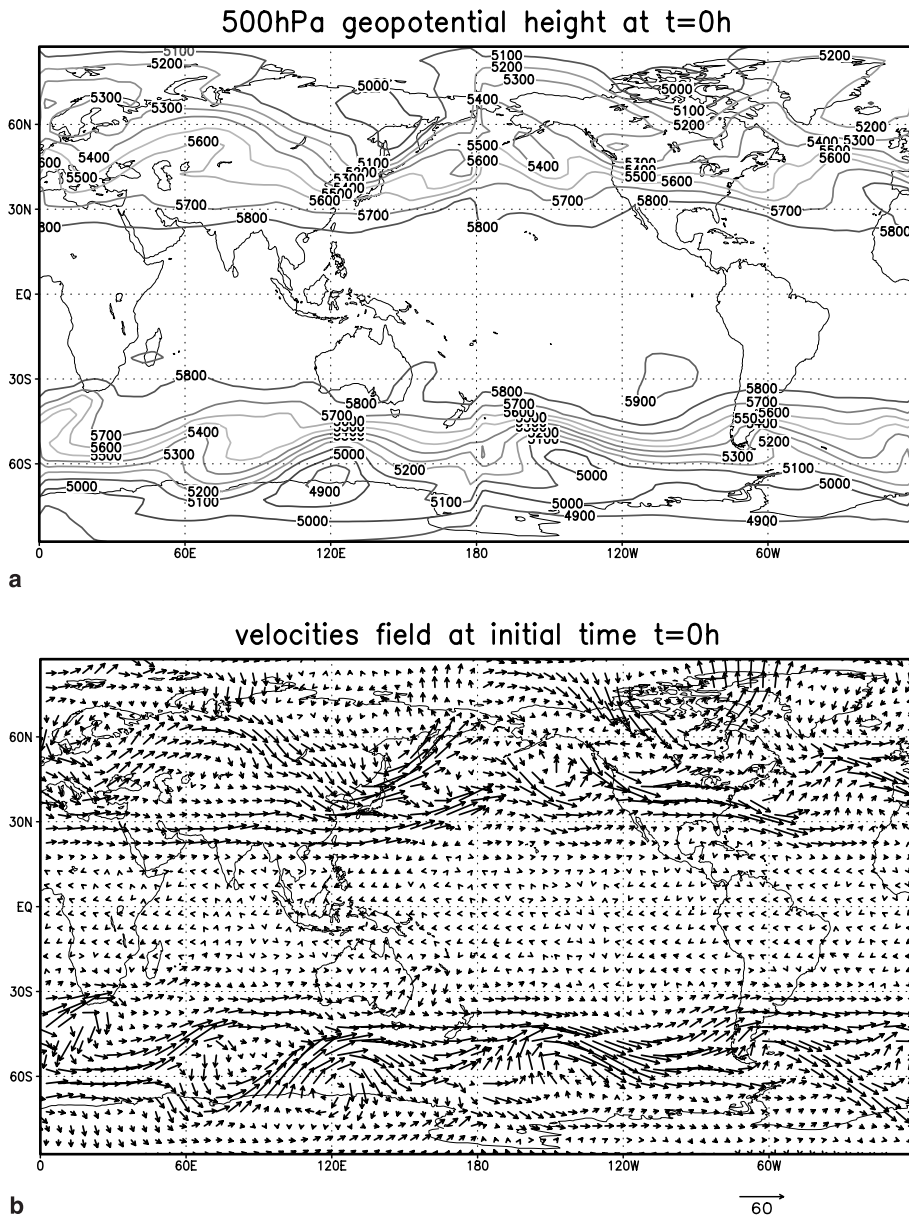


Fig. 1. The configuration of the model state for the reference run (\mathbf{x}_0^{ref}): 500 hPa geopotential height and velocities field at the initial time $t = 0$ h and after a 24 h forecast

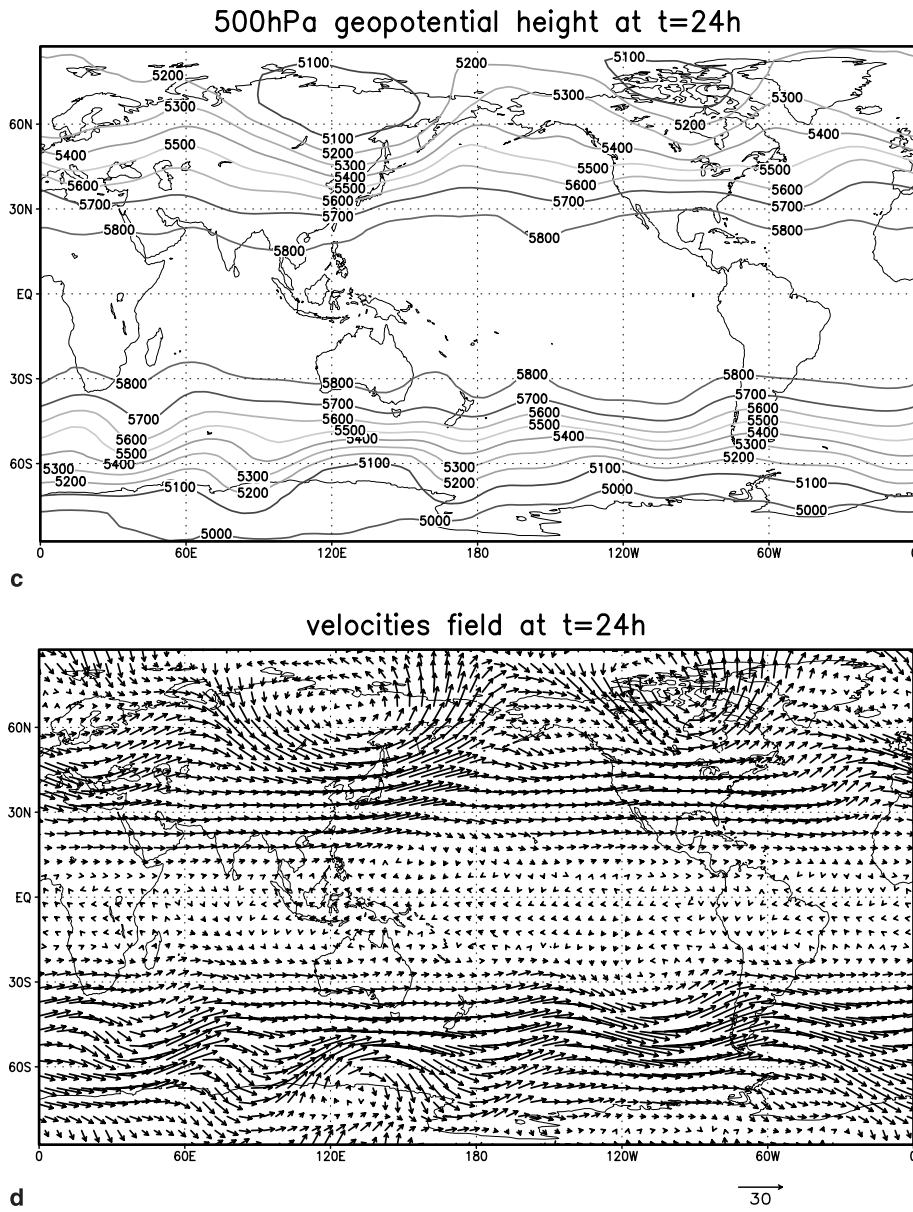


Fig. 1 (continued)

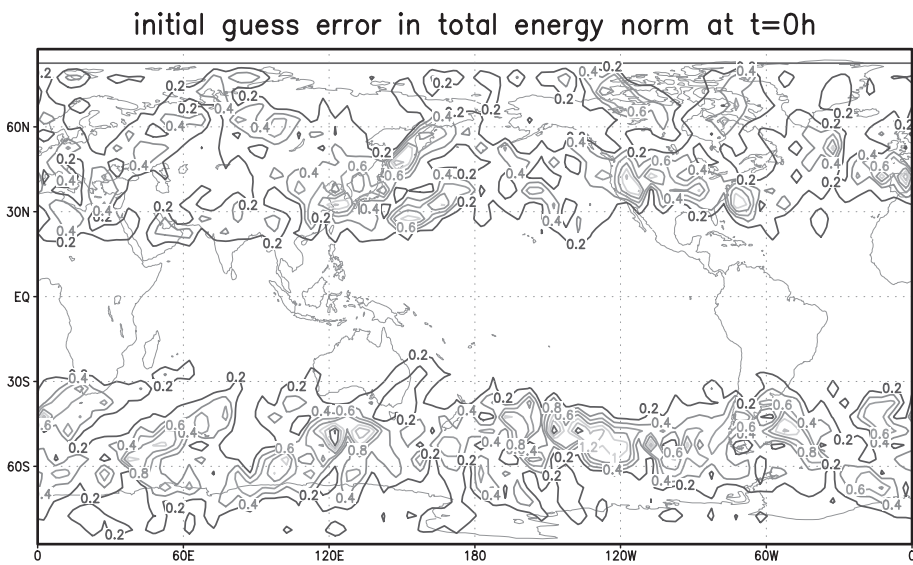


Fig. 2. Distribution of the error $\mathbf{x}^b - \mathbf{x}_0^{ref}$ in the background estimate of the initial model state. Isoleths of the magnitude of are shown in the total energy norm

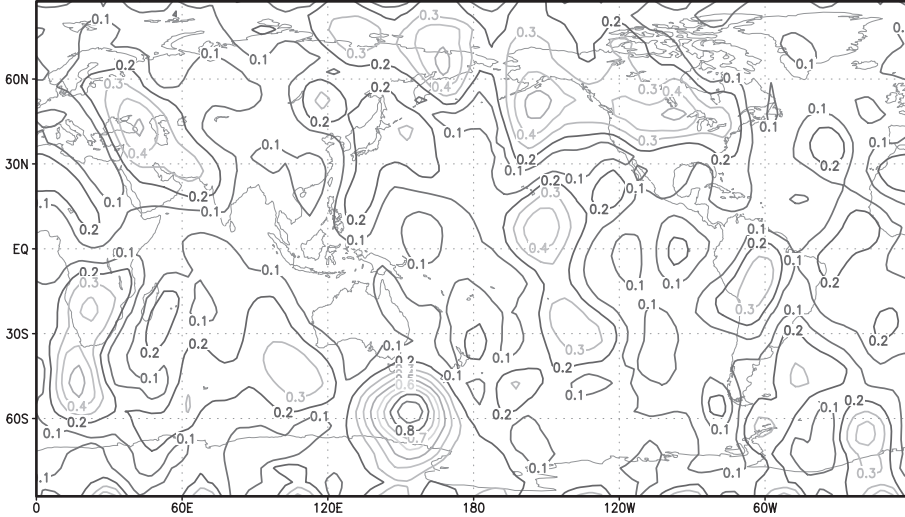
initial guess error in total energy norm at $t=24\text{h}$ 

Fig. 3. Distribution of the forecast error at $t = 24\text{h}$ using the background estimate as the initial condition. Isoleths of the magnitude of are shown in the total energy norm. The largest forecast error is observed over the region $\mathcal{D}_v = [125^\circ\text{E} \ 175^\circ\text{E}] \times [80^\circ\text{S} \ 40^\circ\text{S}]$ which is thus selected as the verification domain

error (t.e. norm) of 24h forecast with fixed obs only

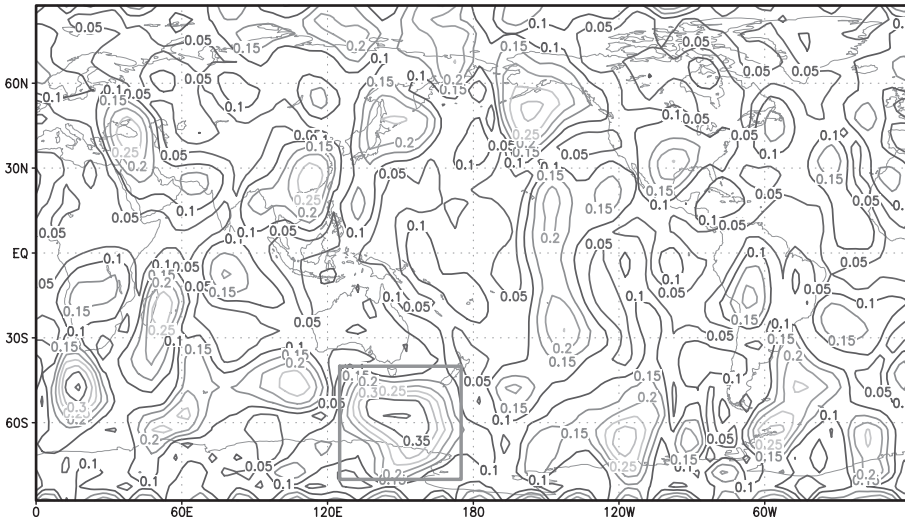


Fig. 4. Distribution of the forecast error in total energy norm at the verification time when data assimilation is performed with observations from fixed locations only ($20^\circ \times 20^\circ$ coarse grid). The verification domain $\mathcal{D}_v = [125^\circ\text{E} \ 175^\circ\text{E}] \times [80^\circ\text{S} \ 40^\circ\text{S}]$ is shown with solid line

an appropriate targeting procedure. In the next section we review two traditional adjoint-based targeting methods: the singular vectors and the adjoint sensitivity.

4. Singular vectors and adjoint sensitivity

Implementation of the adjoint-based targeting methods relies on the linearization of the non-linear forecast model. The intimate relationship between the adjoint (gradient) sensitivity and singular vectors is discussed by Rabier et al (1996). If we consider a perturbation $\delta\mathbf{x}_i$ of the model state at t_i then, to first-order approximation, the

induced perturbation at t_v is expressed as

$$\delta\mathbf{x}_v = \mathcal{M}(\mathbf{x}_i + \delta\mathbf{x}_i) - \mathcal{M}(\mathbf{x}_i) \approx \mathbf{L}(t_i, t_v)\delta\mathbf{x}_i, \quad (7)$$

where $\mathbf{L}(t_i, t_v)$ is the resolvent of the tangent linear model in the optimization interval $t_v - t_i$. On the tangent phase space we consider an inner product

$$\langle \delta\mathbf{x}, \delta\mathbf{y} \rangle_C = \langle \delta\mathbf{x}, \mathbf{C}\delta\mathbf{y} \rangle, \quad (8)$$

where \mathbf{C} is a symmetric positive definite matrix (usually taken to be diagonal), and $\langle \cdot, \cdot \rangle$ is the Euclidean inner product. The adjoint operator of \mathbf{L} in $\langle \cdot, \cdot \rangle_C$ is defined as

$$\langle \mathbf{L}^{*C} \delta\mathbf{x}, \delta\mathbf{y} \rangle_C = \langle \delta\mathbf{x}, \mathbf{L}\delta\mathbf{y} \rangle_C \quad (9)$$

such that $\mathbf{L}^{*C} = \mathbf{C}^{-1}\mathbf{L}^*\mathbf{C}$, where \mathbf{L}^* is the adjoint operator of \mathbf{L} in $\langle \cdot, \cdot \rangle$.

4.1 The singular vectors approach

The singular vectors approach to targeting observations (Palmer et al, 1998; Buizza and Montani, 1999) searches for the directions where errors in the state vector at the targeting time will propagate most at the verification time on the verification domain. From Eq. (9) it follows that

$$\|\delta\mathbf{x}(t_v)\|_C = \langle \delta\mathbf{x}(t_i), \mathbf{L}^{*C}\mathbf{L}\delta\mathbf{x}(t_i) \rangle_C \quad (10)$$

such that the directions characterized by maximum relative growth $\|\delta\mathbf{x}(t_v)\|_C/\|\delta\mathbf{x}(t_i)\|_C$ are the singular vectors $\nu_j(t_i)$

$$\mathbf{L}^{*C}\mathbf{L}\nu_j(t_i) = \sigma_j^2\nu_j(t_i) \quad (11)$$

associated with the largest singular values σ_j .

The singular vectors (11) depend on the C-norm selection. Palmer et al (1998) show that the analysis error covariance metric (AECM) is an optimal choice to improve the forecast skill. In variational data assimilation the Hessian of the cost functional may be used to obtain an approximation of the analysis error covariance matrix. The studies of Barkmeijer et al (1998; 1999) performed in a 3D-Var data assimilation context show that if the operator \mathbf{C} at the initial time is specified to be the Hessian matrix of the cost functional of the variational data assimilation, then the computed singular vectors (HSV) are consistent with 3D-Var estimates of analysis error statistics. The total energy metric corresponds to a diagonal matrix \mathbf{C} and is often used to facilitate the practical implementation. Among other simple metrics, the total energy metric has the advantage that the spectra of the associated dominant singular vectors (TESV) is consistent with the spectra of estimates of the analysis error variance (Palmer et al, 1998).

If \mathbf{P} denotes the projection operator on \mathcal{D}_v , the singular value problem

$$[\mathbf{C}^{\frac{1}{2}}\mathbf{P}\mathbf{L}\mathbf{C}^{-\frac{1}{2}}]^*\mathbf{C}^{\frac{1}{2}}\mathbf{P}\mathbf{L}\mathbf{C}^{-\frac{1}{2}}\mu_j = \sigma_j^2\mu_j, \quad (12)$$

$$\nu_j = \mathbf{C}^{-\frac{1}{2}}\mu_j \quad (13)$$

must be solved in the optimization interval $t_v - t_i$.

Iterative solvers (see, e.g., ARPACK package, Lehoucq et al, 1998) may be used to evaluate the singular values and the associated singular vectors. For large-scale atmospheric models this is an intensive computational process and in practice only 4 to 10 leading singular vectors are used to define the target area as we explain next.

4.1.1 Target area definition using N leading singular vectors

To identify the target area at the targeting time t_i we follow the approach of Buizza and Montani (1999). Consider the first N leading singular vectors $\nu_j, j = 1, 2, \dots, N$ at t_i with unit C-norm, $\|\nu_j\|_C = 1, j = 1, 2, \dots, N$ and let $f_j^C(\lambda, \theta)$ denote the value of the C-norm of ν_j at grid point (λ, θ) (e.g., total energy norm at (λ, θ)). A sensitivity function is defined as

$$F_N^C(\lambda, \theta) = \sum_{j=1}^N \left(\frac{\sigma_j}{\sigma_1} \right) f_j^C(\lambda, \theta). \quad (14)$$

Additional observations taken at t_i at the locations where the sensitivity field (14) is maximal are believed to be of significant benefit for the forecast improvement. The target area is defined as

$$\mathcal{D}_i = \{(\lambda, \theta) | F_N^C(\lambda, \theta) \geq 0.5F_{\text{MAX}}\},$$

$$F_{\text{MAX}} = \max_{(\lambda, \theta)} F_N^C(\lambda, \theta) \quad (15)$$

and adaptive observations locations at t_i are selected as the first n_i locations (λ, θ) where $F_N^C(\lambda, \theta)$ attains the largest values.

The computational cost of implementing targeting methods using singular vectors is significantly increased when multiple targeting instants are considered since for each $t_i, i = 1, 2, \dots, I$ a new set of singular vectors must be computed.

4.2 The adjoint sensitivity approach

In the adjoint sensitivity approach adaptive observations are selected using the gradient of a functional \mathcal{J}_v defined in terms of the forecast at the verification time. Ideally, we would like to evaluate the sensitivity of the forecast error (2) with respect to the model state at the targeting time. A large sensitivity value indicates that small variations in the model state will have a significant impact on the forecast at the verification time.

For practical applications (e.g., flight planning) the functional \mathcal{J}_v must be based on the forecast alone since the forecast error at t_v is not known at the planning time. Some of the difficulties related to the operational use and the implementation of the targeting strategies in a real-time framework are discussed by Baker and Daley (2000), and Langland et al (1999). The sensitivity of the average lower-troposphere vorticity was used during FASTEX to select targeted observations (Langland et al, 1999).

Valuable insight on the benefits and shortcomings of targeted observations may be obtained by performing a posteriori (“after-the-fact”) studies. In this case we may consider \mathcal{J}_v to be the cost functional (2) representing the forecast error at t_v . The sensitivity field is defined as

$$F_v(\lambda, \theta) = \|\nabla \mathcal{J}_v^C(\lambda, \theta)\|_C, \quad (16)$$

where $\nabla \mathcal{J}_v^C$ is the gradient of the verification functional. Corresponding to (2) we have

$$\nabla \mathcal{J}_v^C(\mathbf{x}_i) = \mathbf{L}^{*C} \mathbf{P}(\mathbf{x}_v^f - \mathbf{x}_v^{ref}). \quad (17)$$

Adaptive observations at t_i are deployed at the first n_i locations (λ, θ) where $F_v(\lambda, \theta)$ has largest values. Identification of the target area at distinct instants in time proceeds backward from t_I to t_1 and an efficient evaluation of all $\nabla \mathcal{J}_v^C(\mathbf{x}_i)$, $i = 1, 2, \dots, I$ is obtained through a single adjoint model integration. The adjoint sensitivity method may be therefore implemented at a reduced computational cost even in the case when multiple targeting instants are considered.

5. Interactive adaptive observations

Baker and Daley (2000) noticed that traditional targeting methods based on the a priori evaluation of a forecast sensitivity field are completely ignorant of the characteristics of the data assimilation system. Using the adaptive methods described in the previous section optimal adaptive observations at t_i have been determined assuming that these are *the only* available observations. Since 4D-Var data assimilation takes into consideration *all* observations available in the assimilation window, the interaction between observations must be considered by the targeting procedure. In particular, the following question should be addressed: If individually each of \mathcal{O}_i^a at t_i , $i = 1, 2, \dots, I$ is an optimal adaptive

observations set, is $\mathcal{O}^a = \{\mathcal{O}_1^a, \mathcal{O}_2^a, \dots, \mathcal{O}_I^a\}$ still optimal? Bishop (2000) shows with a simple example that an attempt to globally search for an optimal solution from the set of all feasible adaptive observations paths may easily lead to a problem which is computationally impractical. Therefore, even for practical applications of moderate complexity, a serial observations processing must be considered.

The new adjoint sensitivity approach we describe in this section takes into consideration the interaction between adaptive observations at distinct instants in time and the interaction with routine observations. The selection algorithm proceeds backward in time and adaptive observations \mathcal{O}_i^a are selected in a sequential manner. A periodic update of the sensitivity field at t_i is performed to account for all observations already located at t_{i+1} as follows: denote by

$$\mathcal{O}_{i+1} = \mathcal{O}^f \cup \mathcal{O}_I^a \cup \dots \cup \mathcal{O}_{i+1}^a \quad (18)$$

the set of all fixed observations and all adaptive observations already located in the time interval $[t_{i+1}, t_I]$ and consider $\mathcal{J}_{\mathcal{O}_{i+1}}(\mathbf{x}_i)$ the cost functional (1) restricted to the observational set \mathcal{O}_{i+1} as a function \mathbf{x}_i . We introduce a new sensitivity field associated to the observations set \mathcal{O}_{i+1}

$$F_i(\lambda, \theta) = \|\nabla \mathcal{J}_{\mathcal{O}_{i+1}}(\lambda, \theta)\|_C \quad (19)$$

and update the sensitivity field F_v at t_i according to

$$F_v(\lambda, \theta) = F_v(\lambda, \theta) \left(1 + \alpha \frac{F_i(\lambda, \theta)}{F_v(\lambda, \theta)} \right)^{-1}. \quad (20)$$

The updated sensitivity field is inversely proportional to the relative value of the sensitivity field provided by the set of observations that have been already located. Optimal sites for deploying adaptive observations at t_i are now selected at the locations where the sensitivity field (20) has the largest magnitude. Therefore, new observations at t_i are located in regions where the sensitivity of \mathcal{J}_v to the model state is large *and* little additional information may be obtained from *all previously located* observations. The interaction between observations is controlled by the weight coefficient $\alpha > 0$ which reflects our confidence in the previously selected observations (e.g., observational errors).

The sensitivity field F_i may be evaluated at once for all $i = I, I-1, \dots, 1$ by periodically

updating the observational set (18) during the adjoint model integration. The additional computational cost is roughly given by the computational cost of a backward integration in the assimilation window $[t_0, T]$. In practice the length assimilation window is much smaller than the length of the time interval $[t_0, t_v]$ such that the computational overhead required by the update (19)–(20) is relatively small compared to the evaluation of the sensitivity field (16). The benefits of the new approach to targeting observations are presented next in a comparative analysis with both the adjoint sensitivity and singular vectors methods.

Remark. Since the sensitivity field (19) depends on the observations, the update (19)–(20) may be used only for a posteriori targeting applications. However, the method may be easily extended for “a priori” estimates, by defining the functional $\mathcal{J}_{\mathcal{O}_{i+1}}(\mathbf{x}_i)$ only in terms of the forecast at the locations (λ, θ) determined by \mathcal{O}_{i+1} , in a similar manner as \mathcal{J}_v . This approach was presented in the recent work of Daescu and Carmichael (2003).

6. Numerical experiments

In this section, targeting strategies using the leading total energy singular vectors (TESV), adjoint

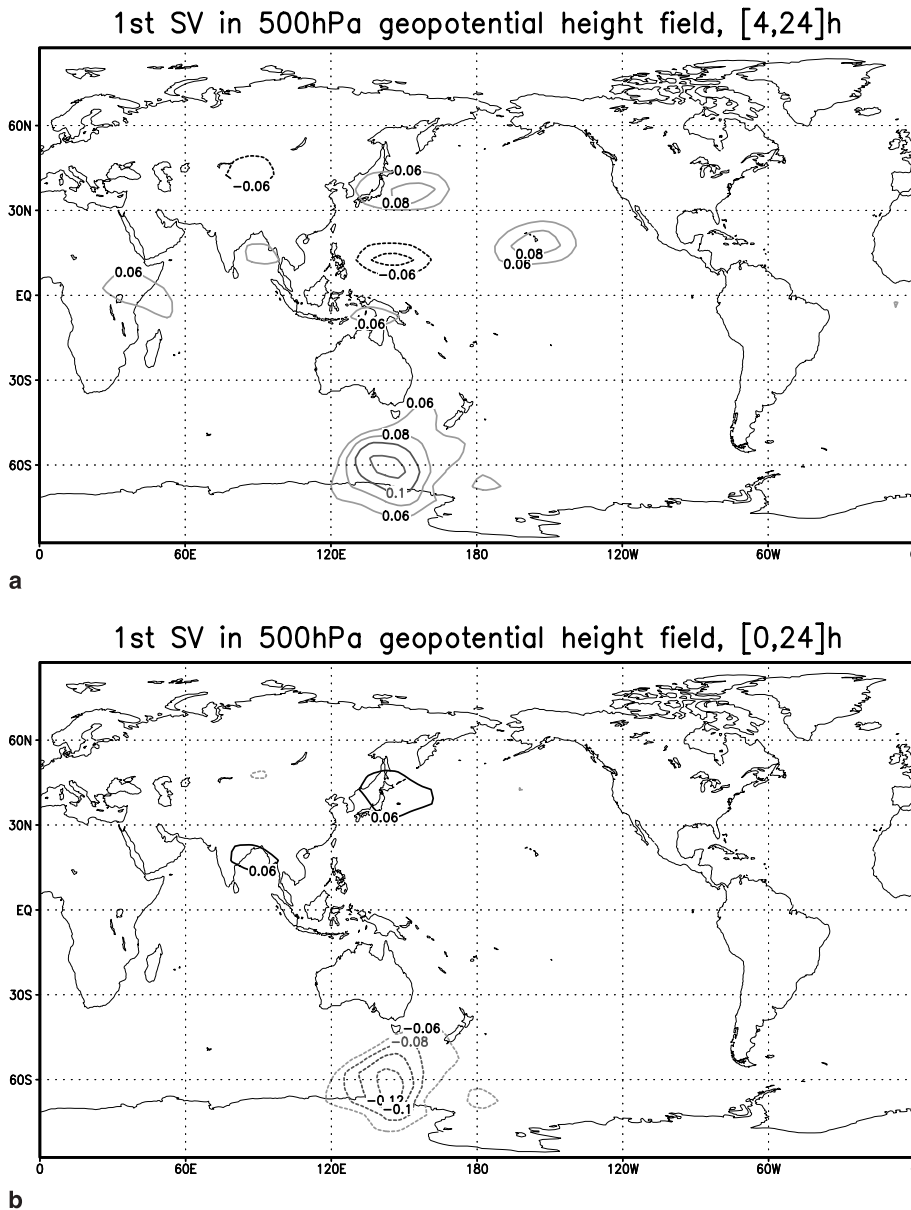


Fig. 5. Time evolution of the first singular vector in 500 hPa geopotential height field for the optimization interval $[t_i, 24 \text{ h}]$. Results shown for $t_i = 0 \text{ h}, 2 \text{ h}, 4 \text{ h}, 6 \text{ h}$

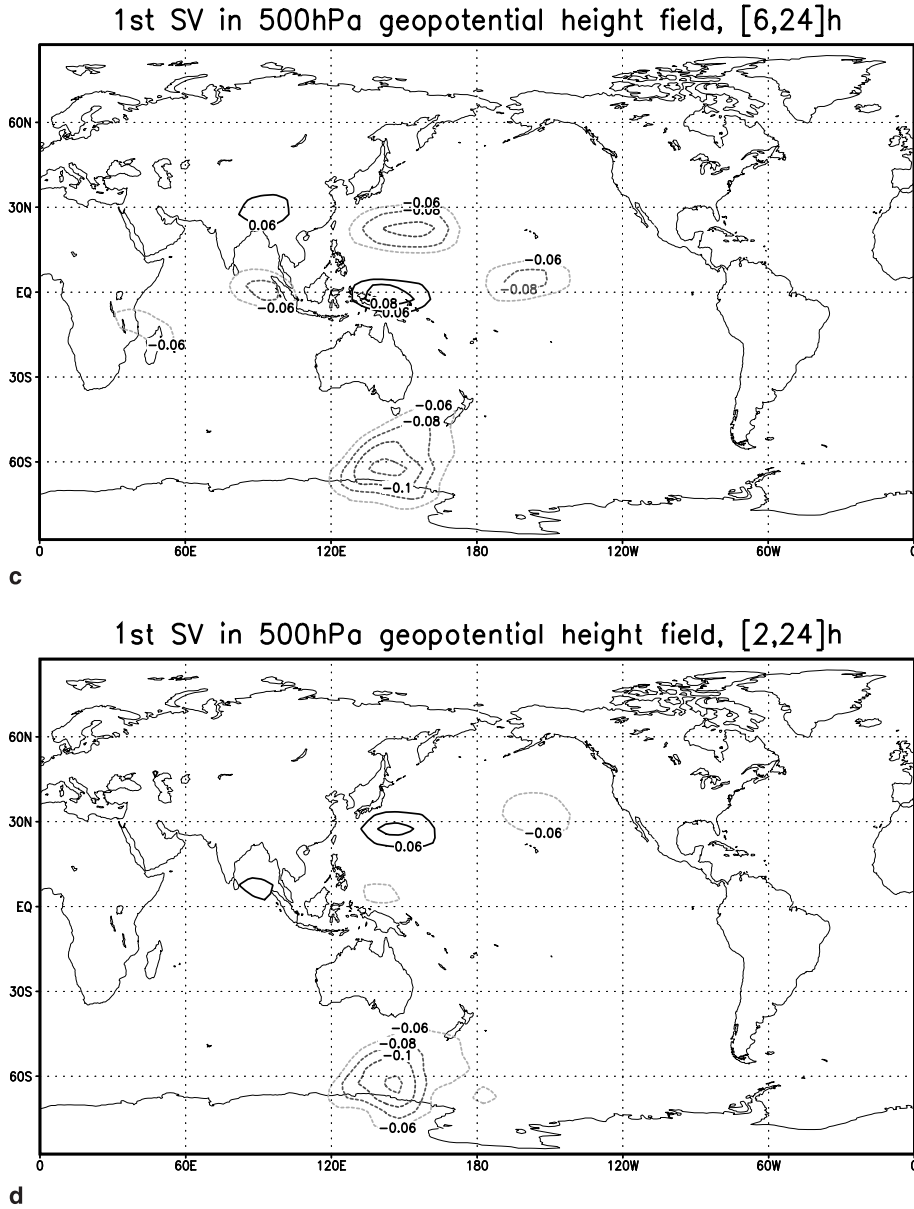


Fig. 5 (continued)

sensitivity (AS), and adjoint sensitivity with interactions between observations (IAS) are analyzed for the shallow-water model and the experimental settings described in Sect. 3. We assume that each hour in the assimilation window $[0, 6\text{h}]$ five adaptive observations must be selected using an appropriate targeting strategy. A comparative performance analysis is presented for two different scenarios: In the first experiment (E1) we assume that the adaptive observations are the only observations available to the data assimilation process ($\mathcal{O}^f = \emptyset$). In the second experiment (E2) we assume that routine

observations are also available on a $20^\circ \times 20^\circ$ coarser mesh grid. For each experiment and for each of the targeting methods a new data assimilation procedure is performed using the quasi-Newton limited memory BFGS minimization algorithm (Liu and Nocedal, 1989). The minimization proceeds until the cost functional is reduced to 0.1% of its initial value. For each targeting method, during the minimization process of the cost functional \mathcal{J} (over the entire domain) which provides the initial condition \mathbf{x}_0^a , we also monitor the evolution of the normalized forecast error reduction $\mathcal{J}_v(\mathbf{x}_0^a)/\mathcal{J}_v(\mathbf{x}_0)$ at

$t_v = 24$ h over the verification domain $\mathcal{D}_v = [125^\circ \text{E } 175^\circ \text{E}] \times [80^\circ \text{S } 40^\circ \text{S}]$. The total energy norm is used to define the inner product $\langle \cdot, \cdot \rangle_C$ and to quantify the forecast error (2) at t_v .

To implement the AS and IAS methods we used the gradient fields F_v associated to the verification functional (2) (a posteriori targeting). To implement the TESV method, 10 leading singular values and their associated singular vectors were computed at each targeting instant t_i using the ARPACK package (Lehoucq et al, 1998). The evolution of the first singular vector in 500 hPa

geopotential height field for the optimization interval $[t, 24 \text{ h}]$ with $t = 0 \text{ h}, 2 \text{ h}, 4 \text{ h}, 6 \text{ h}$ is shown in Fig. 5. Similarly, in Fig. 6, we show the time evolution of the first singular vector in zonal wind field. The adjoint model associated with the forward model discretization was generated using the automatic adjoint compiler TAMC (Giering and Kaminski, 1998). The validity of the linear model approximation (7) in the interval $[0, 24 \text{ h}]$ was verified by comparing nonlinearly evolved perturbations (control minus perturbed experiment) with a perturbation evolved using the tangent operator.

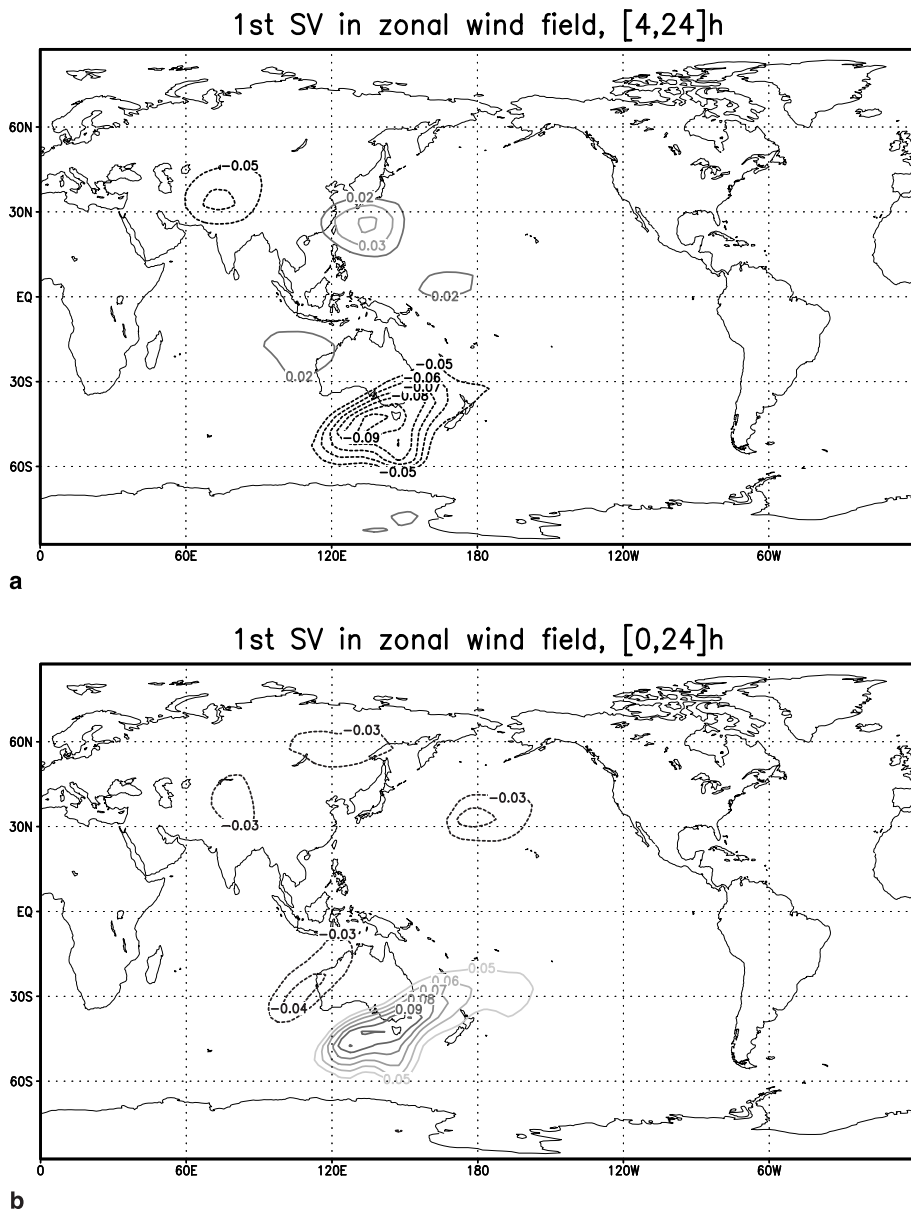


Fig. 6. Time evolution of the first singular vector in zonal wind field for the optimization interval $[t_i, 24 \text{ h}]$. Results shown for $t_i = 0 \text{ h}, 2 \text{ h}, 4 \text{ h}, 6 \text{ h}$

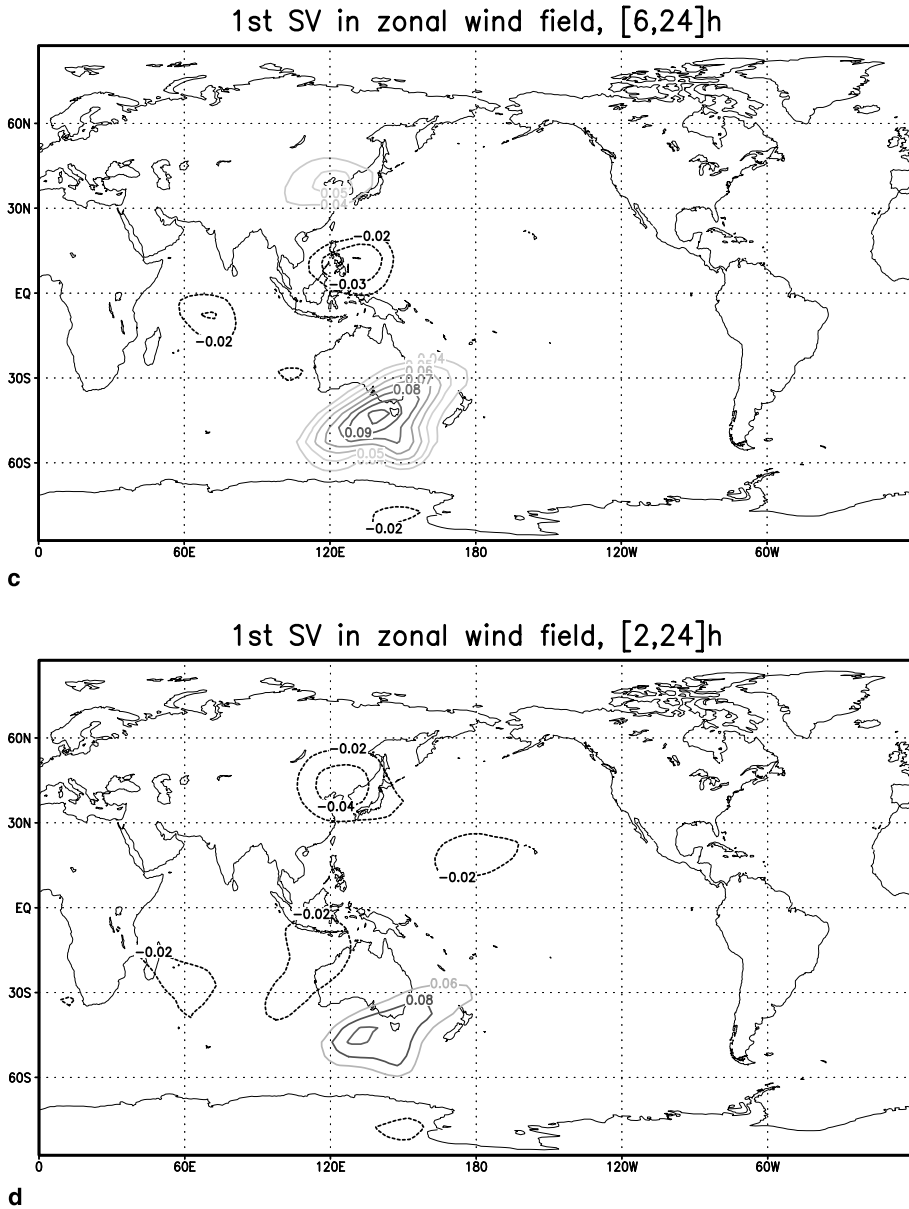


Fig. 6 (continued)

6.1 A comparative analysis of targeting methods

We begin our analysis by presenting the results obtained for the experiment E1 when only adaptive observations are provided to the data assimilation. The evolution of the sensitivity field obtained with the adjoint sensitivity (AS) method is shown in Fig. 7 for $t_i = 0$ h, 2 h, 4 h, 6 h. The location of the adaptive observations (marked with “ \triangle ” in Fig. 7) corresponds to the grid points where the sensitivity field has the largest magnitude.

The dynamics of the sensitivity field is significantly changed when the interaction between the observations is taken into consideration as we show in Fig. 8 for the IAS targeting method. Adaptive observations using adjoint sensitivity with interaction between observations (IAS) are marked in Fig. 8 with “ \square ”. Locations marked with “ \triangle ” in Fig. 8 were selected also by the previous approach (AS). Since the selection of the adaptive observations proceeds backward in time, $t_l = 6$ h is the first targeting instant. At this time no observations were previously located

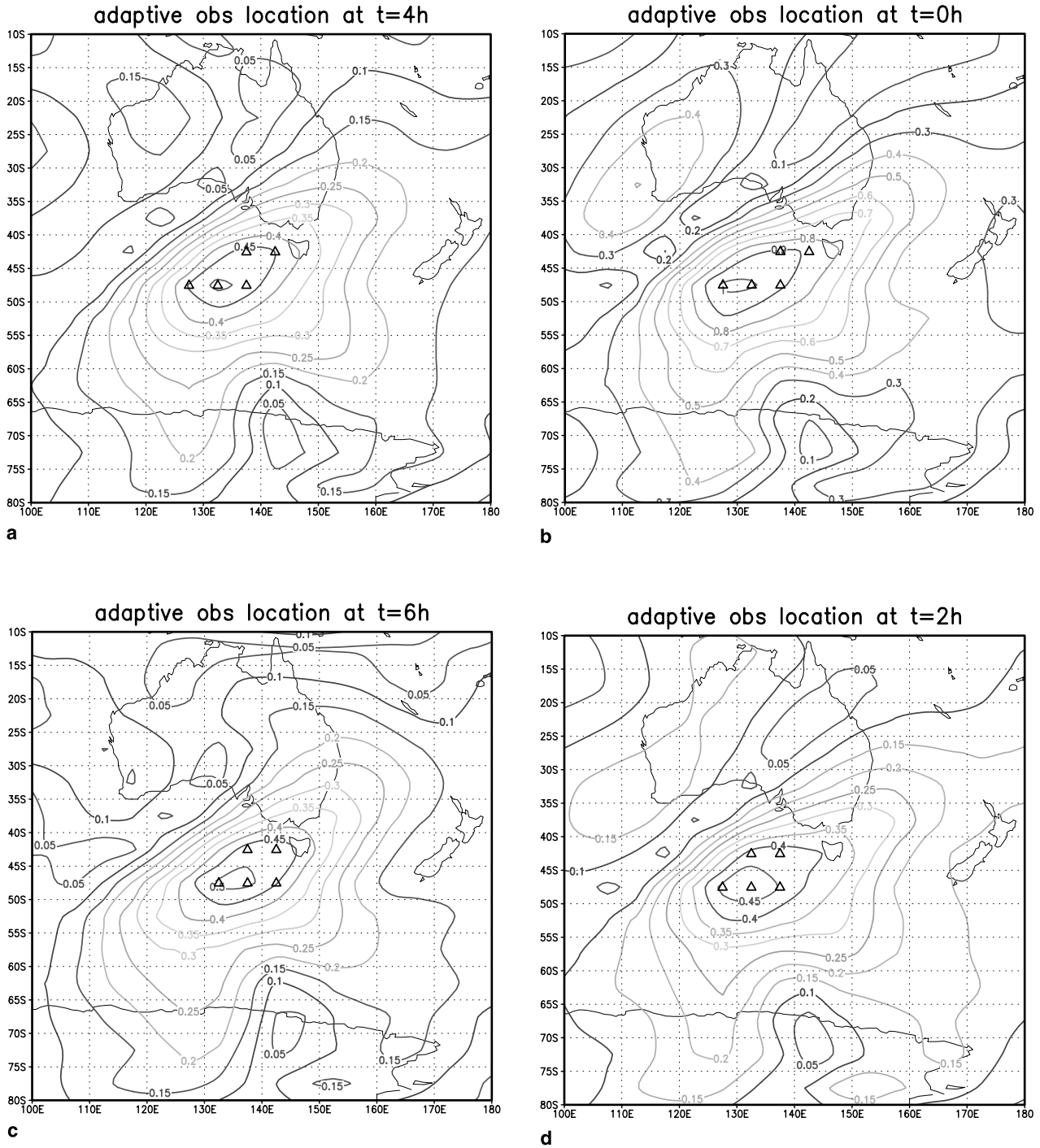


Fig. 7. Time evolution of the sensitivity field corresponding to the adjoint sensitivity method (AS). Results shown for $t_i = 0$ h, 2 h, 4 h, 6 h. The location of the adaptive observations at t_i is marked with “ Δ ” and corresponds to the grid points where the sensitivity field has the largest magnitude

such that the sensitivity fields are identical and both AS and IAS methods selected the same set of observations. To identify new locations at the following targeting instants, the IAS method takes into consideration the influence of all

observations already located. From Figs. 7 and 8 we notice that the periodical update of the sensitivity field results in less spatial clustering for the adaptive observations. The IAS method searches to identify regions where the magnitude

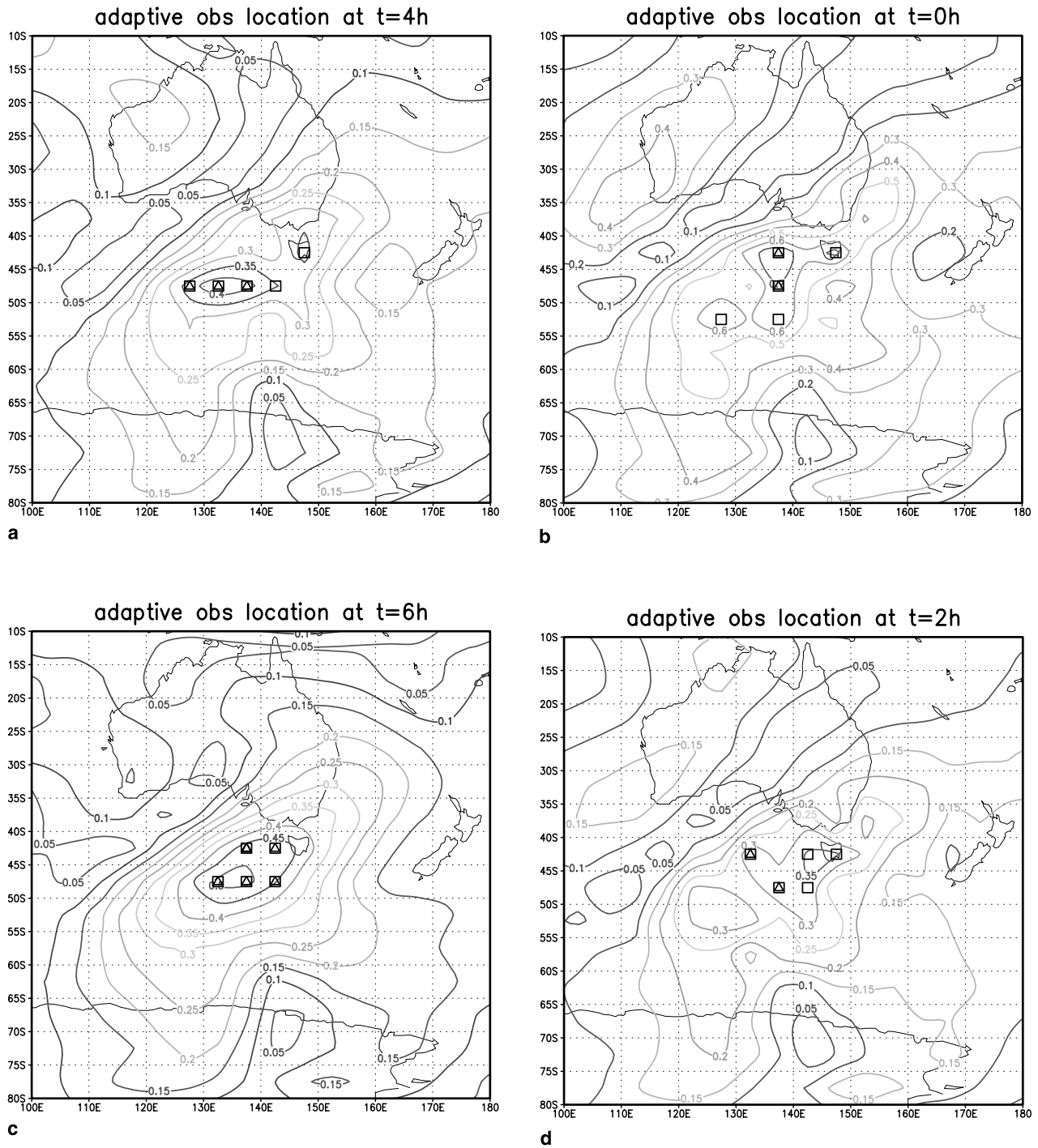


Fig. 8. Time evolution of the sensitivity field corresponding to the adjoint sensitivity method with interaction between observations (IAS). Results shown for $t_i=0h, 2h, 4h, 6h$. The location of the adaptive observations selected by the IAS method at t_i is marked with " \square ". Locations marked with " \triangle " were also selected by the AS method (Fig. 7)

of the sensitivity field is large, conditioned by the information accumulated from previously located observations.

The evolution of the sensitivity field corresponding to the total energy singular vectors

method is shown in Fig. 9, and the location of the adaptive observations is marked with " \circ ". For each targeting method, the distribution of the forecast error at the verification time over the verification domain after data assimilation

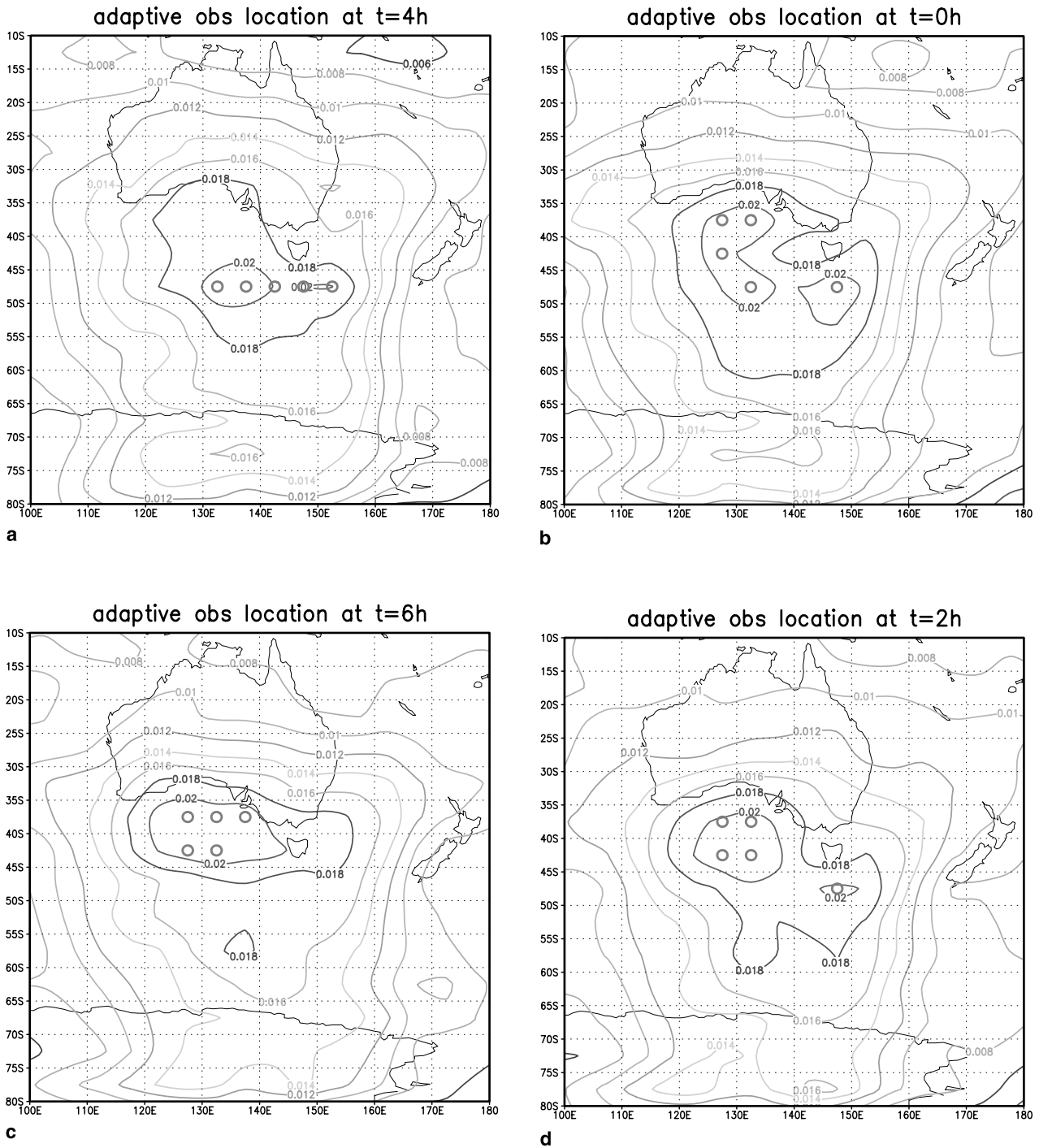


Fig. 9. Time evolution of the sensitivity field and adaptive observations location (marked with "o") using the leading singular vectors method (TESV). Results shown for $t_i = 0$ h, 2 h, 4 h, 6 h

takes place is shown in the total energy norm in Fig. 10. The forecast error using the background estimate as initial conditions is also displayed in Fig. 10. At each iteration during the minimization process of the cost functional \mathcal{J} we monitor the forecast improvement using

targeted observations by evaluating the ratio $\mathcal{J}_v(\mathbf{x}_0^a)/\mathcal{J}_v(\mathbf{x}_0)$. The results displayed in Fig. 11 show that the targeting method using interactive adaptive observations outperforms the adjoint sensitivity as well as the singular vectors targeting methods.

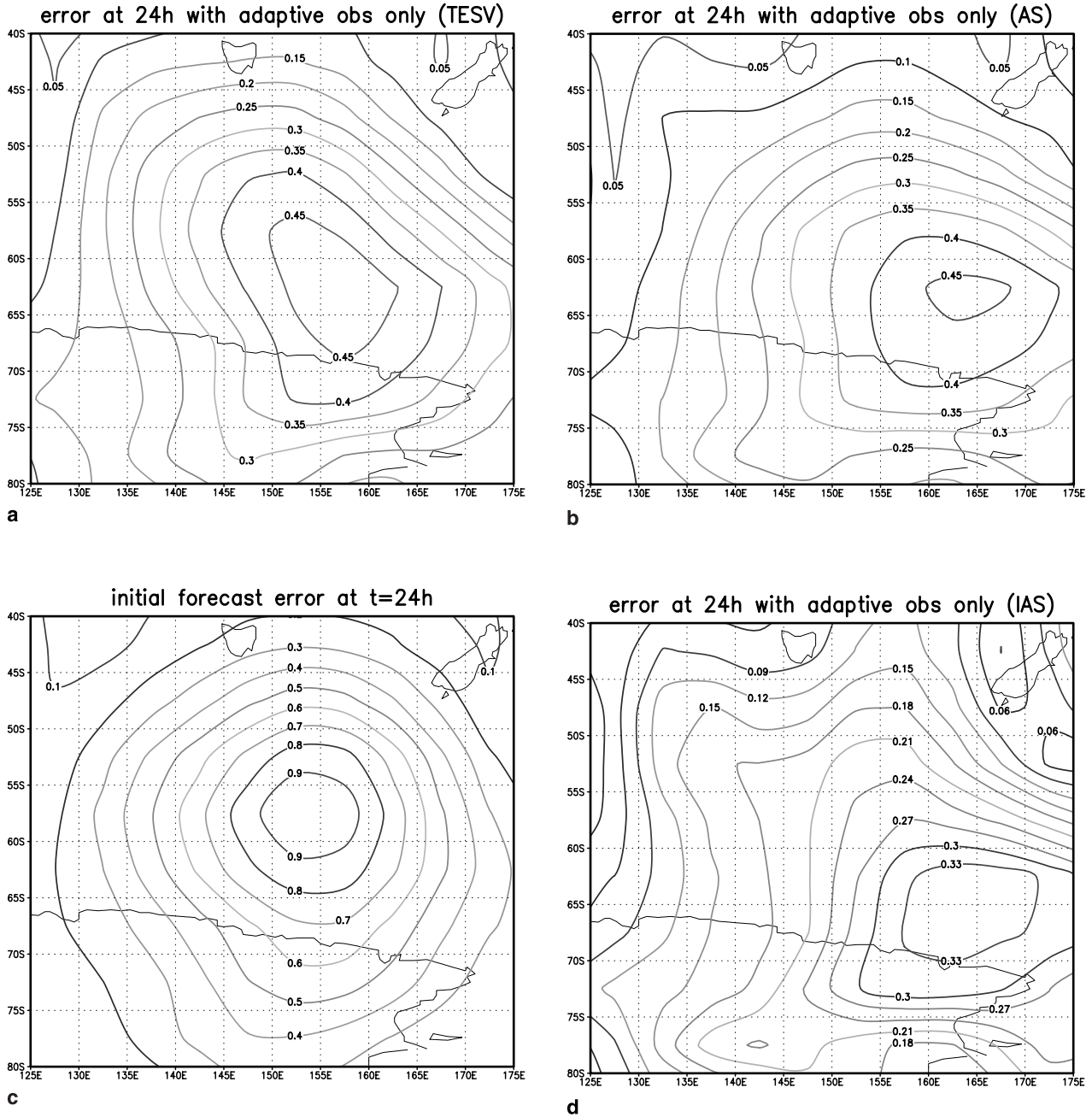


Fig. 10. Distribution of the forecast error at the verification time over the verification domain when data assimilation is performed using adaptive observations only. For reference, the error in the forecast initiated from the background estimate is also displayed. Isoleths of the magnitude are shown in the total energy norm

Next we analyze the forecast improvement for the second scenario, E2, when both routine and adaptive observations are provided to the data assimilation. The benefits of using adaptive observations are evaluated by comparison with an assimilation procedure using only routine observations. Four data assimilation experiments were performed with observations provided as

follows: fixed observations only, fixed and adaptive observations using singular vectors, fixed and adaptive observations using adjoint sensitivity, fixed and adaptive observations using adjoint sensitivity with interaction between observations. For each experiment, the minimization process and the forecast error reduction $\mathcal{J}_v(\mathbf{x}_0^a)/\mathcal{J}_v(\mathbf{x}_0)$ during the minimization of the corresponding

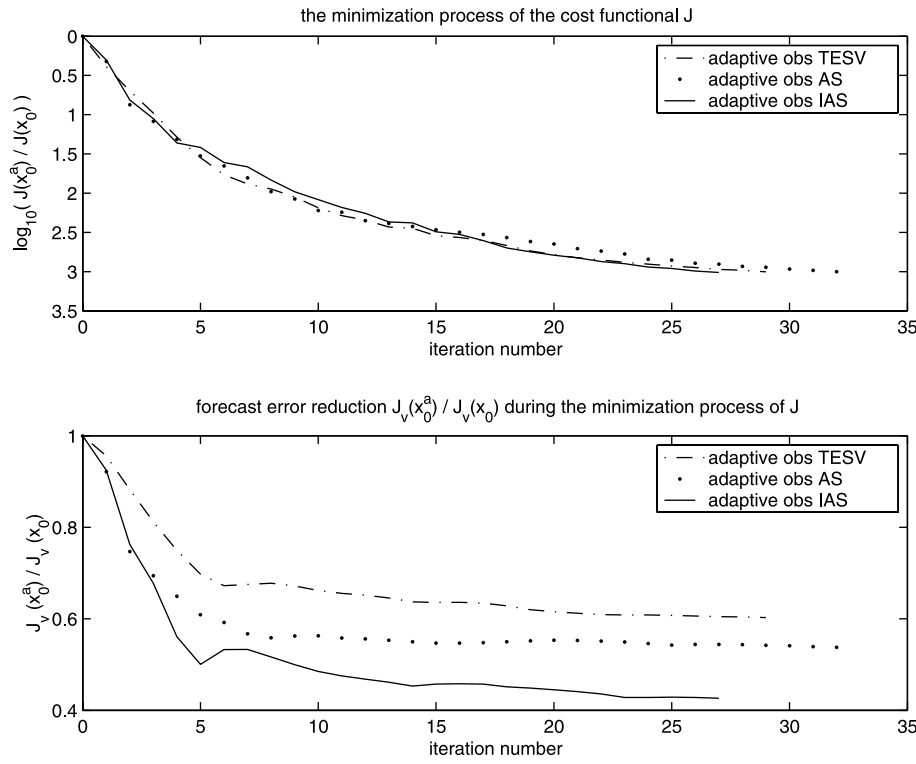


Fig. 11. Top: The minimization of the cost functional \mathcal{J} when only adaptive observations corresponding to TESV, AS, and IAS targeting methods are assimilated. Normalized values are shown on a logarithmic scale. Bottom: During the iterative process, for each targeting method the forecast error reduction at the verification time over \mathcal{D}_v is quantified by evaluating the ratio $\mathcal{J}_v(\mathbf{x}_0^a) / \mathcal{J}_v(\mathbf{x}_0)$

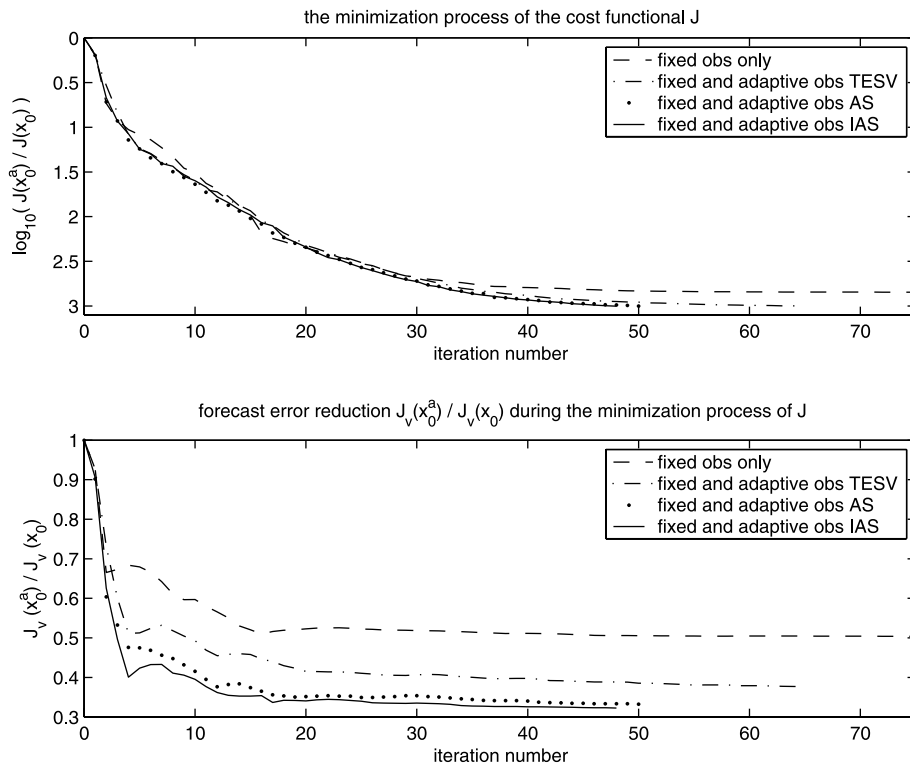
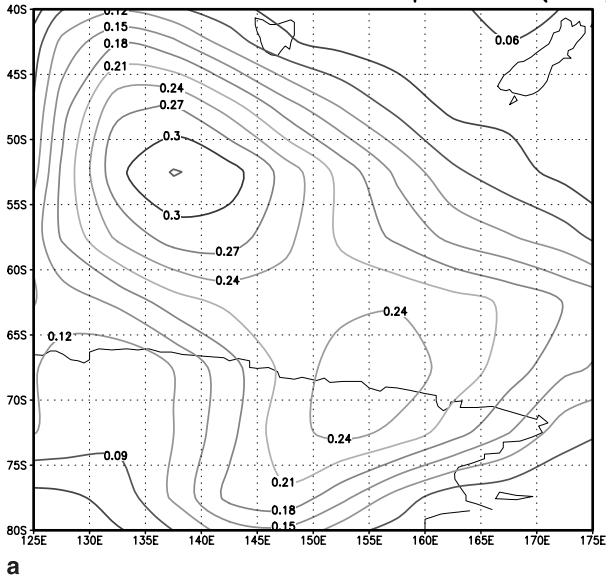


Fig. 12. Top: The minimization of the cost functional \mathcal{J} when both routine and adaptive observations provided by the TESV, AS, and IAS targeting methods respectively, are assimilated. Normalized values are shown on a logarithmic scale. Bottom: During the iterative process, for each targeting method the forecast error reduction at the verification time over \mathcal{D}_v is quantified by evaluating the ratio $\mathcal{J}_v(\mathbf{x}_0^a) / \mathcal{J}_v(\mathbf{x}_0)$. For reference, the results obtained using routine observations only are also displayed

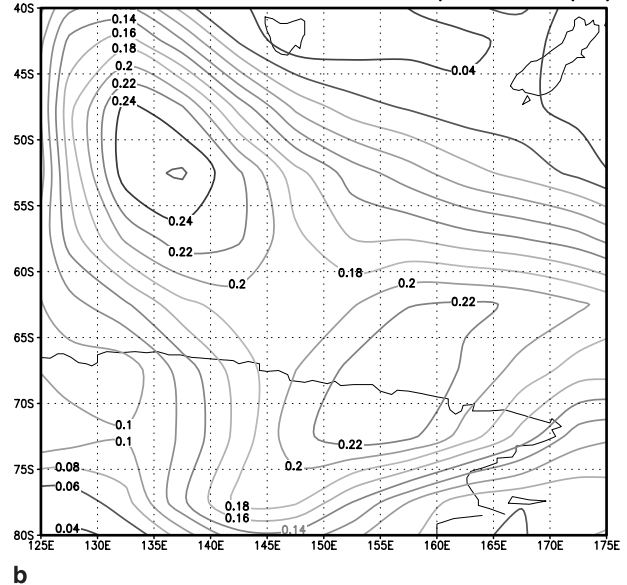
cost functional \mathcal{J} are shown in Fig. 12. The distribution of the forecast error at the verification time over the verification domain is displayed in Fig. 13.

The potential forecast improvement using adaptive observations is limited by various factors such as the accuracy of the background estimate, the configuration of the existing

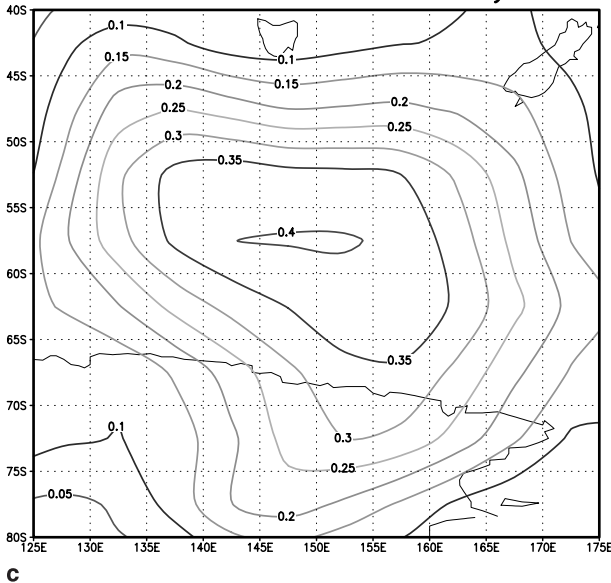
error at 24h with fixed and adaptive obs (TESV)



error at 24h with fixed and adaptive obs (AS)



error at 24h with fixed obs only



error at 24h with fixed and adaptive obs (IAS)

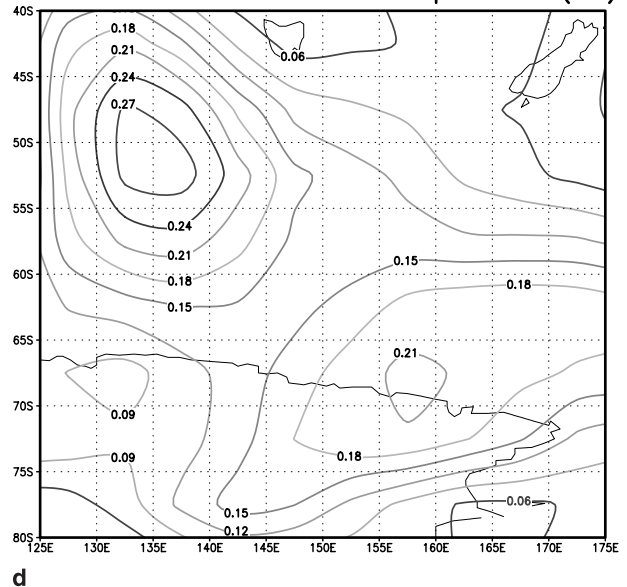


Fig. 13. Distribution of the forecast error at the verification time over the verification domain when data assimilation is performed using both routine and adaptive observations provided by the TESV, AS, and IAS targeting methods, respectively. For reference, the results obtained using routine observations only are also displayed

observational network, and the number of additional observational resources allocated. In Fig. 12, it can be seen that the adaptive method using the interaction between observations still provided the best forecast over \mathcal{D}_v , but there is only little improvement as compared to the adjoint sensitivity method.

Remark. One should notice that by using adaptive observations we only attempt to improve the forecast over a given sub-domain at a given future time. In Fig. 14, we show the distribution of the forecast error at 24h over the entire domain after data assimilation using fixed and interactive adaptive observations takes place.

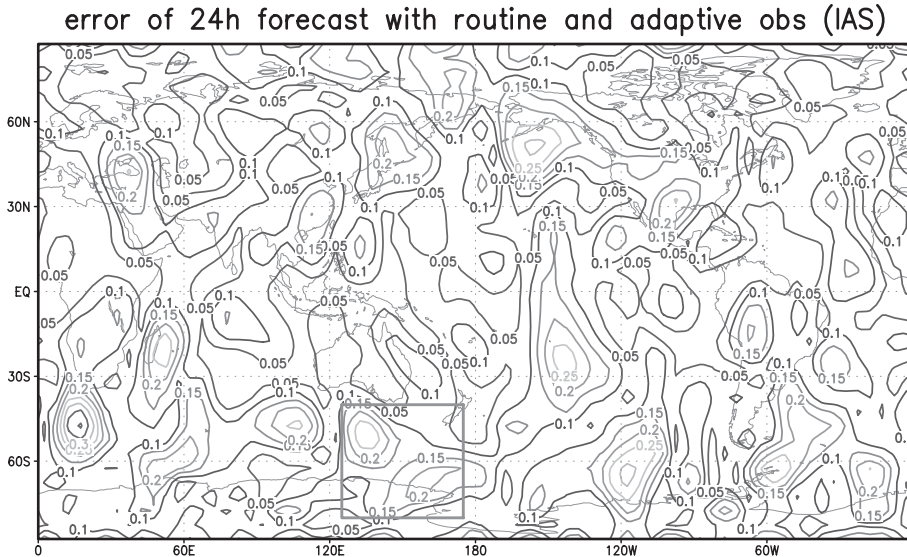


Fig. 14. Distribution of the forecast error in total energy norm at the verification time when data assimilation is performed with routine and adaptive observations provided by the IAS targeting method. Significant forecast improvement may be observed over the verification domain (see also Figs. 3 and 4)

By comparison with Fig. 4, it can be seen that adaptive observations have significant benefits on the forecast over the verification domain $\mathcal{D}_v = [125^\circ \text{E } 175^\circ \text{E}] \times [80^\circ \text{S } 40^\circ \text{S}]$, and little or no forecast improvement is observed outside this region.

7. Conclusions and further research

In this study the adaptive observations problem is presented in the context of 4D-Var data assimilation. It is emphasized that to fully account for the temporal dimension of the 4D-Var scheme, multiple targeting instants must be considered in the assimilation window. Our work represents a first step in the design of optimal sampling strategies for time distributed adaptive observations. In particular, it is shown that the interaction between targeted observations taken at distinct instants in time has a significant impact on the efficiency of the adaptive strategies.

A new adjoint sensitivity approach for adaptive observations is proposed which takes into consideration the interaction between adaptive observations at distinct instants in time and their interaction with routine observations. The main difference between the proposed method and the traditional adjoint sensitivity approach consists in the dynamic update of the sensitivity field associated with the verification functional. To perform this update, a new sensitivity field is used to quantify the information accumulated at the targeting time from all previously located

observations. A simple interaction mechanism is designed such that new adaptive observations are located in regions where the sensitivity of the forecast to the model state is large and little additional information may be obtained from all previously located observations. The additional computational cost is given by a backward integration of the adjoint model in the assimilation window such that the method is feasible to implement for large scale applications. No claim is made that the proposed approach provides an optimal adaptive observational path among all feasible sets of observations. However, our analysis presented for a global 2D shallow-water model shows that the new targeting method may be used to provide an improved model forecast as compared to the total energy singular vectors and the adjoint sensitivity targeting methods.

Given the potential impact to improve the models forecasts and the multitude of practical applications, significant research remains to be done to develop optimal adaptive observations techniques. Our future research will focus on the implementation of targeting methods using interactive adjoint sensitivity fields for comprehensive operational atmospheric models. A rigorous theoretical framework to account for time distributed adaptive observations remains to be formulated.

In the adjoint method described in this paper targeted observations are identified backward in time, starting from the end of the assimilation window. Since from a theoretical point of view

the least uncertainty is at the shortest lead time, a natural approach is to design a forward marching adaptive method. In the 4D-Var context, a decision must be made at t_0 for the entire adaptive observational path, such that the influence of the targeted observations located at $t_1 > t_0$ on targeted observations at $t_2 > t_1$ must be 'a priori' estimated. The main difficulty in this case is to find an efficient way to forward propagate the information provided by the location of targeted observations. A forward marching targeting algorithm based on a similar updating technique may be implemented if we assume that at each targeting instant t_i , N_i possible deployments of additional observations are a priori specified. A comparative analysis between the forward/backward marching targeting algorithms will be presented in our future work. We will also investigate the application of interactive sensitivity fields to targeting methods using singular vectors and ensemble forecasts. The sensitivity to observations technique proposed by Baker and Daley (2000) may be extended to the 4D-Var data assimilation to analyze the interaction between the existing observational network, the background estimate of the model state, and adaptive observations.

Further adaptive observations studies should also consider the availability of worldwide remote sensing observations that are typically not used in the routine data assimilation (e.g., GPS, satellite radiances of massively multiple channel sensors, cloudy radiances) in conjunction with aircraft deployed targeted observations.

Acknowledgements

The first author acknowledges the support from the Supercomputing Institute for Digital Simulation and Advanced Computation of the University of Minnesota. The second author acknowledges the support from the School of Computational Science and Information Technology, Florida State University and from the NSF grant number ATM-0201808 managed by Dr. Linda Peng whom he would like to thank for her support.

References

Baker NL, Daley R (2000) Observation and background adjoint sensitivity in the adaptive observation-targeting problem. *Quart J R Meteorol Soc* 126: 1431–1454
 Barkmeijer J, Van Gijzen M, Bouttier F (1998) Singular vectors and estimates of the analysis-error covariance metric. *Quart J R Meteorol Soc* 124: 1695–1713

Barkmeijer J, Buizza R, Palmer TN (1999) 3D-Var Hessian singular vectors and their potential use in the ECMWF Ensemble Prediction System. *Quart J R Meteorol Soc* 125: 2333–2351
 Bergot T (2001) Influence of the assimilation scheme on the efficiency of adaptive observations. *Quart J R Meteorol Soc* 127: 635–660
 Berliner LM, Lu Z-Q, Snyder C (1999) Statistical design for adaptive weather observations. *J Atmos Sci* 56: 2536–2552
 Bishop CH (2000) Estimation theory and adaptive observing techniques. *Quart J R Meteorol Soc* (submitted)
 Bishop CH, Toth Z (1999) Ensemble transformation and adaptive observations. *J Atmos Sci* 56: 1748–1765
 Bishop CH, Etherton BJ, Majumdar SJ (2001) Adaptive sampling with the ensemble transform Kalman filter. Part I: Theoretical aspects. *Mon Wea Rev* 129: 420–436
 Buizza R, Montani A (1999) Targeted observations using singular vectors. *J Atmos Sci* 56: 2965–2985
 Corazza M, Kalnay E, Patil DJ, Yorke JA, Hunt BR, Szunyogh I, Cai M (2002) Use of the breeding technique in the estimation of the background error covariance matrix for a quasi-geostrophic model. Preprints of the AMS Symp. on Observations, Data Assimilation and Probabilistic Prediction, 13–17 January 2002, Orlando, Florida, pp 154–157
 Courtier P, Thepaud JN, Hollingsworth A (1994) A strategy of operational implementation of 4D-Var using an incremental approach. *Quart J R Meteorol Soc* 120: 1367–1388
 Daescu DN, Carmichael GR (2003) An adjoint sensitivity method for the adaptive location of the observations in air quality modeling. *J Atmos Sci* 60(2): 434–450
 Daley R (1991) Atmospheric data analysis. Cambridge University Press, 457pp
 Doerenbecher A, Bergot T (2001) Sensitivity to observations applied to FASTEX cases. *Nonlinear Proc Geophys* 8: 467–481
 Giering R, Kaminski T (1998) Recipes for adjoint code construction. *ACM T Math Software* 24(4): 437–474
 Giraldo FX, Neta B (1995) Software for the staggered and unstaggered Turkel-Zwas schemes for the shallow water equations on the sphere. NPS-MA-95-008, Technical Report Naval Postgraduate School, Monterey, CA.
 Hansen JA, Smith LA (2000) The role of operational constraints in selecting supplementary observations. *J Atmos Sci* 57(17): 2859–2871
 Jazwinski AH (1970) Stochastic processes and filtering theory. Academic Press, 376pp
 Joly A and coauthors (1999) The Fronts and Atlantic Storm-Track Experiment (FASTEX): Scientific objectives and experimental design. *Bull Amer Meteorol Soc* 78: 1917–1940
 Kalnay E (2002) Atmospheric modeling, data assimilation and predictability. Cambridge Univ. Press, 512pp
 Kalnay E, Park SK, Pu Z-X, Gao J (2000) Applications of the quasi-inverse method to data assimilation. *Mon Wea Rev* 128: 864–875
 Langland R, Rohaly G (1996) Adjoint-based targeting of observations for FASTEX cyclones. Preprints, 7th Conf.

- on Mesoscale Process, Reading, UK, Amer Meteor Soc 369–371
- Langland RH, Gelaro R, Rohaly GD, Shapiro MA (1999) Targeted observations in FASTEX: Adjoint-based targeting procedures and data impact experiments in IOP17 and IOP18. *Quart J R Meteorol Soc* 125: 3241–3270
- Langland RH, Toth Z, Gelaro R, Szunyogh I, Shapiro MA, Majumdar SJ, Morss RE, Rohaly GD, Velden C, Bond N, Bishop CH (1999) The North Pacific Experiment (NORPEX-98): Targeted observations for improved North American weather forecasts. *Bull Amer Meteorol Soc* 80: 1363–1384
- Lehoucq RB, Sorensen DC, Yang C (1998) ARPACK User's Guide: Solution of large-scale eigenvalue problems with implicitly restarted Arnoldi methods. *Software, Environments, and Tools* 6, SIAM, 160pp
- Leutbecher M, Barkmeijer J, Palmer TN, Thorpe AJ (2002) Potential improvement of forecasts of two severe storms using targeted observations. *Quart J R Meteorol Soc* 128(583): 1641–1670
- Liu DC, Nocedal J (1989) On the limited memory BFGS method for large scale minimization. *Math Prog* 45: 503–528
- Lorenz EN, Emanuel KA (1998) Optimal sites for supplementary weather observations: Simulation with a small model. *J Atmos Sci* 55: 399–414
- Majumdar SJ, Bishop CH, Buizza R, Gelaro R (2002) A comparison of PSU-NCEP ensemble-transform Kalman-filter targeting guidance with ECMWF and NRL total-energy singular-vector guidance. *Quart J R Meteorol Soc* 128(585): 2527–2549
- Morss RE, Emanuel KA, Snyder C (2001) Idealized adaptive observation strategies for improving numerical weather prediction. *J Atmos Sci* 58: 210–234
- Navon IM, de Villiers R (1987) The application of the Turkel-Zwas explicit large time step scheme to a hemispheric barotropic model with constraint restoration. *Mon Wea Rev* 115(5): 1036–1051
- Neta B, Giraldo FX, Navon IM (1997) Analysis of the Turkel-Zwas scheme for the two-dimensional shallow water equations in spherical coordinates. *J Comp Phys* 133(1): 102–112
- Palmer TN, Gelaro R, Barkmeijer J, Buizza R (1998) Singular vectors, metrics, and adaptive observations. *J Atmos Sci* 55: 633–653
- Pu Z-X, Kalnay E (2000) Targeting observations with the quasi-inverse linear and adjoint NCEP global models: performance during FASTEX. *Quart J R Meteorol Soc* 125: 3329–3337
- Rabier F, Klinker E, Courtier P, Hollingsworth A (1996) Sensitivity of forecast errors to initial conditions. *Quart J R Meteorol Soc* 122: 121–150
- Szunyogh I, Toth Z, Morss RE, Majumdar SJ, Etherton BJ, Bishop CH (2001) The effect of targeted dropsonde observations during the 1999 winter storm reconnaissance program. *Mon Wea Rev* 128: 3520–3537
- Toth Z, and coauthors (2002) Adaptive observations at NCEP: Past, present and future. Preprints of the Symp. on Observations, Data Assimilation and Probabilistic Prediction, 13–17 January 2002, Orlando, Florida (forthcoming)
- Williamson DL, Drake JB, Hack JJ, Jakob R, Swarztrauber PN (1992) A standard test set for numerical approximations to the shallow water equations in spherical geometry. *J Comp Phys* 102: 211–224

Authors' addresses: D. N. Daescu, Institute for Mathematics and its Applications, University of Minnesota, 400 Lind Hall, 207 Church Street S.E., Minneapolis, MN 55455, USA; I. M. Navon, Dept. of Mathematics and School of Computational Science and Information Technology, Florida State University, Tallahassee, FL 32306-4120, USA